


Coexistence of turbulence regimes in the Texas Helimak


Cite as: Phys. Plasmas **28**, 032301 (2021); <https://doi.org/10.1063/5.0033381>

Submitted: 15 October 2020 . Accepted: 09 February 2021 . Published Online: 09 March 2021

 F. A. C. Pereira,  D. L. Toufen,  Z. O. Guimarães-Filho,  I. L. Caldas,  R. L. Viana, and K. W. Gentle

COLLECTIONS

 This paper was selected as Featured

 This paper was selected as Scilight



[View Online](#)



[Export Citation](#)



[CrossMark](#)



Physics of Plasmas
Features in Plasma Physics Webinars

Register Today!

Coexistence of turbulence regimes in the Texas Helimak

Cite as: Phys. Plasmas **28**, 032301 (2021); doi: [10.1063/5.0033381](https://doi.org/10.1063/5.0033381)

Submitted: 15 October 2020 · Accepted: 9 February 2021 ·

Published Online: 9 March 2021



View Online



Export Citation



CrossMark

F. A. C. Pereira,^{1,2,a)}  D. L. Toufen,³  Z. O. Guimarães-Filho,²  I. L. Caldas,²  R. L. Viana,¹  and K. W. Gentle⁴

AFFILIATIONS

¹Department of Physics of Federal, University of Paraná, 81531-990 Curitiba, Paraná, Brazil

²Institute of Physics, University of São Paulo, 05315-970 São Paulo, São Paulo, Brazil

³Federal Institute of Education, Science and Technology of São Paulo, 07115-000 Guarulhos, São Paulo, Brazil

⁴Department of Physics and Institute for Fusion Studies, The University of Texas at Austin, 78712 Austin, Texas, USA

^{a)} Author to whom correspondence should be addressed: faugusto@if.usp.br

ABSTRACT

The turbulence of magnetically confined plasmas usually presents high-density pulses with short duration known as bursts. In the Texas Helimak, it is possible to suppress bursts in a broader region by applying a negative electrostatic bias. However, an almost unchanged burst rate persists in a region far from the location where bias is applied. We investigate the turbulence transition that occurs from the burst suppressed region to the burst dominated region by analyzing data from Langmuir probes in the whole radial extension of the machine. We find that such turbulence transition can be understood as an alternation of two different turbulent regimes, with the probability of being in each regime depending on the radial position. One regime, named as burst-free regime, consists of only Gaussian fluctuations and the other, named as bursty turbulent regime, is a train of pulses with double exponential temporal profiles, exponential amplitude distribution, and random occurring instants. This succession between burst-free and bursty turbulent regimes influences the equilibrium parameters.

Published under license by AIP Publishing. <https://doi.org/10.1063/5.0033381>

I. INTRODUCTION

One of the biggest challenges to achieve an efficient plasma magnetic confinement in fusion machines is the control of the particles losses due to anomalous transport.¹ The anomalous transport observed at the edge of magnetic confined plasmas is driven by electrostatic turbulence.^{2,3} One of its features is the presence of radially propagating coherent structures that are observed as high-density pulses⁴ with relative short duration, but responsible for a significant component of the plasma edge particles and energy transport.⁵ These density pulses show a convective transport dynamics, which is studied in tokamaks,^{6,7} linear machines,⁸ and Helimaks.^{9–12}

These intermittent high-density pulses, called bursts (also known as blobs or avaloids), are a universal feature present in all magnetically confined plasmas.^{4,9,11,13–17} The burst intermittency has motivated the creation of models that feature bursts trains to describe the plasma fluctuations in the scrape-off layer (SOL) of tokamaks.^{18–20} One of the models considers Lorentzian pulses to explain the exponential power spectra^{15,18} found in some plasma turbulence experiments. In this model, the pulses are generated by chaotic advection due the interaction of drift waves at the edge of confined plasmas.^{15,21}

Another approach models the scrape-off layer (SOL) fluctuations as composed uniquely of self-similar pulses with exponential profile, arriving at random times.¹⁹ This model is able to reproduce the quadratic relation between skewness and kurtosis of the turbulent fluctuations found in many magnetic confined machines.¹⁹ When the burst temporal profiles and arriving frequencies are fitted, this model reproduces well both the power spectrum and histogram of the turbulent signal found in the SOL of plasma machines.^{20,22} However, in the previous analyzed experiences and models, there has been no investigation reporting the transition from a background fluctuations burst-free to a bursty plasma, as observed from the plasma edge to the scrape-off layer in fusion machines.

Helimaks are basic plasma machines with highly reproducible discharges, a large number of electrostatic probes^{11,12,23} and many properties in common with the scrape-off layer region of tokamaks: open magnetic lines and magnetic and flow shears. They present favorable conditions to investigate bursts and their main characteristics.^{10,11} Moreover, the Texas Helimak²³ turbulence can be changed by electrostatic biasing, going from a high turbulence bursty regime to a burst-free regime with much lower turbulence level and Gaussian-like histograms.^{23,24} A better understanding of the transition between those

two turbulence regimes in Texas Helimak deserves further investigation.

In this article, we analyze discharges in Texas Helimak for which the bursty turbulence is suppressed, in the vicinity where the negative biasing was applied, and bursty turbulence remained in the low field side region far from the biasing position. Between these two regions, turbulence behavior changes continuously. Thus, in the same discharges, we analyze the spatial transition from one region with lower turbulence level to another region where the bursty turbulence remained unchanged by the biasing. We find that the spatially turbulence change is well described by a superposition of the two mentioned regimes. Thus, in the analyzed discharges with negative biasing, we are able to investigate such spatial turbulence transition, in contrast with our previous investigations for bursty regime obtained for positive biasing discharges, where burst production is enhanced.²²

We present evidence that the burst-free regime is well described by Gaussian fluctuations around a mean density, while the bursty turbulence can be seen as the stochastic burst train scenario studied in Refs. 19, 20, and 22. The relative contribution of each regime to the signal changes depending on the radial position, going from burst-free the whole time to bursty turbulence all the time. In the transition region, the time intervals in which the plasma remains in each regime seem to have random duration.

In Sec. II, we introduce the Texas Helimak. In Sec. III, we discuss the models applied to describe the plasma turbulence regimes in the Texas Helimak and compare them with experimental data. In Sec. IV, we apply the turbulence models to analyze the transition between turbulence regimes seen in negative biasing experiments. In Sec. V, we discuss the coexistence of burst-free to bursty regime in the same radial position. A summary of the results is presented in Sec. VI.

II. THE TEXAS HELIMAK

The Texas Helimak²³ is a basic plasma machine with toroidal vessel and open helical magnetic field lines having a small vertical slope [Fig. 1(a)]. The simple geometry approximates an infinite sheared cylindrical slab and, thus, the machine presents an

one-dimensional magnetohydrodynamic equilibrium. The plasma is generated by electron cyclotron resonance heating (ECRH), with the injection of microwave in the vessel by a window at the bottom of high field sidewall. The exact resonance radial position can be controlled by changing the electric current in the coils, and thus changing the magnetic field intensity.

The Texas Helimak has four sets of four plates [see Fig. 1(a)], located at the bottom and top of the machine. All the magnetic field lines intercept two of these plates (one at top and the other at the bottom). There is a large array of Langmuir probes mounted on these plates, with a data acquisition system that can collect data from 96 probes simultaneously at 500 ksamples/s for about 10 s.²⁴ The data used in our analyses are ion saturation current signals measured in a large number of radial positions in the whole machine, mounted close to the top of the bottom plates, with a radial resolution of 2 cm.

Besides serving as a mounting surface for the probes, it is possible to apply an electrostatic potential on these plates and change the plasma properties. In the experiments reported here, the bias was applied on the plate set number 2 that has been used as standard bias plate in Texas Helimak studies. Examples of different density radial profiles are shown in Fig. 1(b), corresponding to $V_b = 0$ (the plate set 2 is grounded, as the other sets) and for two perturbed discharges with $V_b = -20$ V and 10 V.

Besides the change in the density profile, it is also established²³ that the electrostatic bias in the Texas Helimak changes the turbulence regime: there is a strong reduction in the turbulence level and a regime with suppression of intermittent bursts is observed²³ when a negative bias is applied. Without biasing, the standard regime in this region is a bursty turbulence, and it is also known^{9,22} that positive biasing increases the amplitude and number of bursts. In Fig. 2, we present examples for the two mentioned turbulence regimes in the radial position $r = 1.11$ m that are obtained by changing the bias values ($V_b = 10$ V for the bursty regime and -20 V for the burst-free regime). Figure 2(a) shows local short time trace of both regimes: bursty in blue continuous line, where we see a trail of similar pulses, and a burst suppressed (or burst-free) regime in dashed black line, for which large

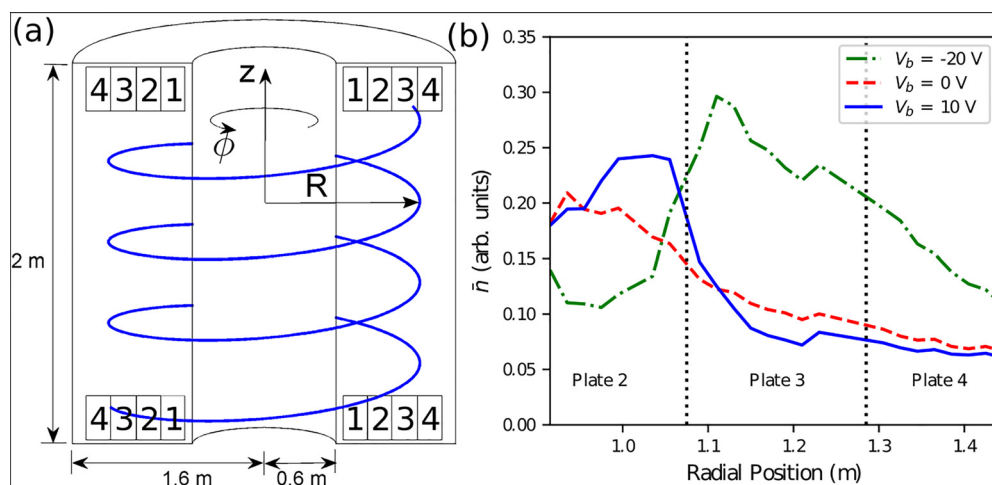


FIG. 1. (a) Texas Helimak vacuum chamber showing an example of the magnetic field lines and the plates used as a support for the Langmuir probes. (b) Density profiles for three different biasing potentials V_b applied on the plate set number 2, with the limit of each plate indicated by dashed vertical lines.

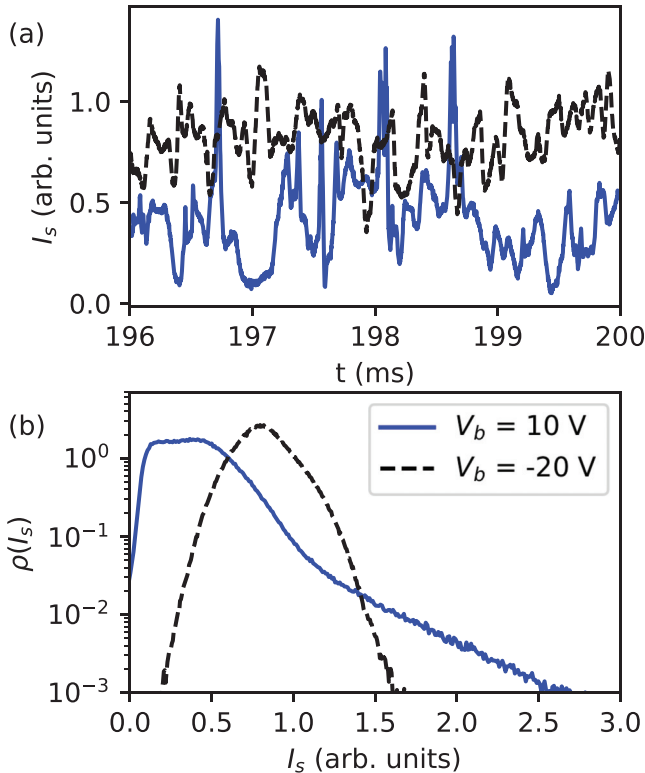


FIG. 2. (a) Example of time series for two biasing potentials (10 V and -20 V) at the same radial position ($r = 1.11$ m), and (b) the histograms of the same time series, with the dashed green and red curves obtained from Eq. (2).

positive peaks do not appear. The respective signal histograms are presented in Fig. 2(b), with the characteristic long tail for large amplitudes for the blue curve, corresponding to the bursts observed with the positive biasing. On the other hand, for the negative biasing, the black Gaussian-like curve indicates the suppression of the intermittent bursts and an increase in the mean plasma density.

III. HELIMAK TURBULENCE REGIMES

In Fig. 3, we show that both bursty and burst suppressed turbulence can be observed in the same plasma discharge according to the radial position of the probe. The burst-free turbulence is observed in a probe close to the place where the bias ($V_b = -20$ V in this discharge) is applied ($r = 1.11$ m, in black), while the bursty regime is observed by a probe at larger radius ($r = 1.425$ m, in blue). The biasing can suppress the burst turbulence in the density gradient region, but in the most external regions, on the fourth plate ($r > 1.3$ m), the biasing effect is much smaller, and the plasma remains in the bursty regime.

The experimental histograms of Fig. 3(b) can be described by considering two different turbulence regimes. One histogram, for the region close to the biasing plate ($r = 1.11$ m), can be described by choosing conveniently the parameters of a Gaussian distribution:

$$\rho_g(I_s) = \frac{1}{\sqrt{2\pi}\sigma} e^{-\frac{(I_s - I_0)^2}{2\sigma^2}}, \quad (1)$$

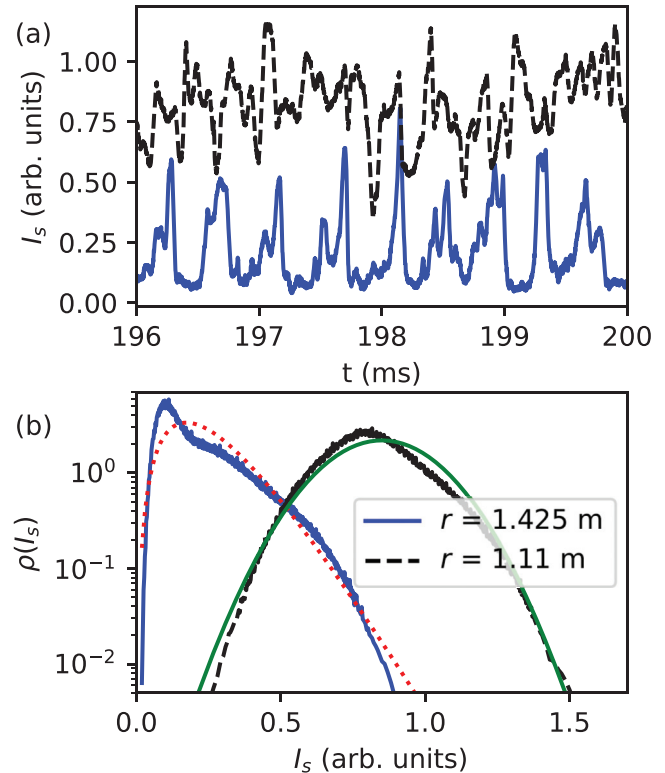


FIG. 3. Time traces (a) and histograms (b) for probes close to the bias plate (black, $r = 1.11$ m) and in the far end of the machine (blue, $r = 1.425$ m), with bias potential of $V_b = -20$ V, with the fitted distributions using Eqs. (1) and (3).

with mean I_0 and standard deviation σ . The resulted fitted histogram is represented by a continuous green line in Fig. 3(b).

The turbulence that generates the blue histogram from Fig. 3(b), for a position far from the biased plate ($r = 1.425$ m), can be described by a stochastic pulse train model,²² similar to those that have been used to describe the burst turbulence observed in tokamaks plasma edge^{19,20} and basic plasma machines

$$I_s(t) = \sum_j A_j p(t - t_j), \quad (2)$$

where I_s is the ion saturation current, which is composed of a trail of pulses that share the same temporal profile, given by the function $p(\tau)$, with random amplitudes A_j and time occurrences t_j . The pulse temporal profile $p(\tau)$, with $\tau = 0$ being the instant which the pulse achieves its maximum value, is double exponential with their amplitude A_j following an exponential distribution [in the Texas Helimak case, the pulse shape $p(t)$ does not follow exactly a double exponential, but the difference can be seen as a second order correction²²].

Under these conditions, the probability distribution function of the signal I_p generated by the bursts superposition is:²⁰

$$\rho_p(I_s) = \frac{I_s^{k-1} e^{-I_s/s}}{s^k \Gamma(k)}, \quad (3)$$

where k is the pulses overlap parameter (the ratio of the pulse characteristic time and the mean time between two consecutive pulses) and s is the scale parameter (the pulse mean amplitude $\langle A_j \rangle$). The result of the fitted histogram can be seen in Fig. 3(b), in a dotted red line. One important note is that sometimes a small background fluctuation, besides the pulse train, may be present in the signal. It usually distorts the bulk of the distribution and has little effect on the exponential tail. We decided to keep the model without a background because it is not necessary to add it to capture the essence of the phenomena. Adding a background noise also increases the number of parameters to fit and the overall complexity of the fitting procedure, without significant gains in the process.

IV. TRANSITION BETWEEN TURBULENCE REGIMES

In the analyzed experiment, the bursts suppression caused by the bias voltage has a limited radial reach, decreasing with the distance from the biased electrode. So, a transition from burst-free turbulence to the bursty one can be found looking at the turbulence signal from probes at different radial positions in the same plasma discharge, as can be seen in Fig. 3(b), with histograms for burst-free and bursty fluctuations at, respectively, $r = 1.11$ m and $r = 1.425$ m, for $V_b = -20$ V. Experimental data from Fig. 4(a) show the radial transition from the burst-free turbulence to a bursty turbulence for a

discharge with bias potential of -20 V, presenting a pronounced bimodal distribution at intermediary radial positions. In Fig. 4(b), we present a heatmap of the histograms according to their radial position, with dashed lines pointing the location of the probes showed in Fig. 4(a) and small arrow pointing the probe positions from Fig. 3.

Figure 4(b) suggests that the transition from burst-free to the bursty turbulence happens with a substitution of one regime for another, as the histogram of a bursty turbulence is substituting the Gaussian one for increasing radial coordinate, generating a discontinuity of distribution maximum and a region with bimodal histograms. This transition cannot be accurately described neither by the distributions given by Eqs. (1) or (3) nor by a sum of the signals of a pulse train with a Gaussian background, because none of these models can generate the observed bimodal distributions of Fig. 4(b). The distribution that arises from the sum of two (independent) variables is the convolution of their distributions. The Gaussian distribution is strongly unimodal, and the distribution from Eq. (3) (a gamma distribution) is always unimodal, thus their convolution is always unimodal.²⁵

The bimodal distribution shapes and the way the transition happens (Fig. 4) indicate that the distributions in the transition region seem like linear combinations of the Eqs. (1) and (3) distributions

$$\rho(I_s) = P_b \rho_p(I_s) + (1 - P_b) \rho_g(I_s), \quad (4)$$

where ρ_g is the Gaussian probability density function (PDF), from Eq. (1), and ρ_p is the exponential burst model distribution from Eq. (3). Furthermore, the model is consistent with an alternation of these two turbulent regimes, burst-free and bursty, with the signal spending certain amount of time in each, and P_b being the fraction of time the signal stays in the bursty turbulence. The two turbulence regimes [Eqs. (1) and (3)] are limit cases of this model that can be obtained when P_b approaches either 0 or 1.

In this model, the transition between these two regimes can be recognized by the appearance of bimodal PDFs, as observed in Fig. 4(a). Then, the model parameters were estimated from the histograms by a nonlinear least squares fitting of the PDFs by Eq. (4).

An example of the fitted distribution is shown in Fig. 5(a), for $r = 1.25$ m and $V_b = -20$ V, corresponding to the dashed line histogram from Fig. 4(a), with the contribution of each component also shown separately. It can be seen that the observed maximum at small I_s and the exponential tail for higher values of I_s are due the bursty distribution component, while the maximum with larger I_s is mainly due the Gaussian term (burst-free regime). In Fig. 5(b), we show the mean values of the experimental signal and of each individual component, bursty and Gaussian. The experimental signal mean value mainly follows the Gaussian component (burst-free regime) for smaller radius and the bursty regime for larger ones, smoothly changing from one to the other regime mean value in the transition region. It is interesting to notice that the mean density value of the Gaussian component is higher than the bursty one for the whole interval.

Figure 6(a) shows the fraction parameter P_b as a function of the radial position and the biasing potential. Here, it is possible to see how the regime transition is affected by the change of biasing: from a bursty-dominated turbulence everywhere when $V_b = 0$ V, to a burst-free regime, for $V_b = -20$ V, in the density gradient region ($r < 1.23$ m) while the data from probes at larger radius are still bursty dominated when there is a negative biasing.

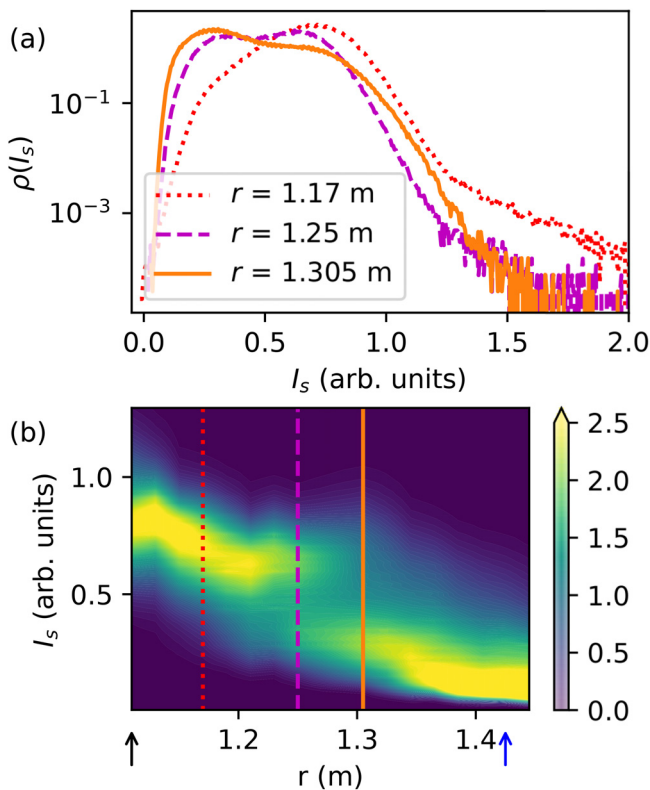


FIG. 4. (a) Examples of experimental histograms in the transition region showing the bimodal characteristic of the distributions with bias potential of -20 V. (b) A 2D heatmap showing the radial dependence of the histograms in plates 3 and 4, with the color showing the probability density, the lines indicate the respective histograms from (a), and the small arrows indicate the two positions from Fig. 3.

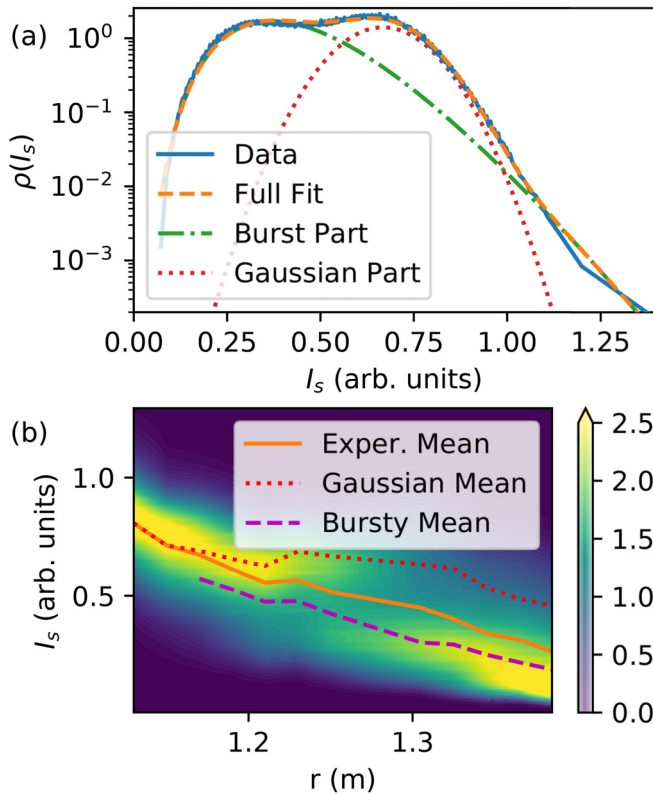


FIG. 5. (a) Example of fitted histogram, for bias potential of -20 V and radius of 1.25 m, using Eq. (4), with the contribution of each term also shown. (b) The radial dependence of the mean values of the experimental signal (solid line), Gaussian part (dotted line), and bursty part (dashed line) of the model fitted from the data. The heat map from Fig. 4(b) in the background.

These regime transitions are very reproducible in the Texas Helimak and, moreover, are also observed with respect to changes in other plasma parameters. For instance, by changing the magnetic field magnitude, the position of the density peak changes, as it moves the ECR heating radial position. Figure 6(b) shows the fraction parameter P_b as function of the radius and the toroidal magnetic field at the machine center (the procedure to change demagnetic field intensity keeps the field line inclinations unchanged). In this scale of magnetic field variation, the effect is only a slight change of the radius where the regime transition occurs, without changing the whole scenario in any significant way. Considering that each bias potential and each magnetic field line are measured in different shots, Fig. 6 also asserts that the reported transition scenario is rather robust.

V. COEXISTENCE OF REGIMES

The results so far on how the transition between regimes happens spatially suggests that inside the transition region, there should be alternating moments of bursty and burst-free regimes. In order to verify this, as there is no simple indicator of bursty regime besides the relatively rare high density bursts, we separated the time series in short time data windows and estimated the windowed fraction parameter $P_b^{(w)}$. In all windows, we assume that the parameters of each regime

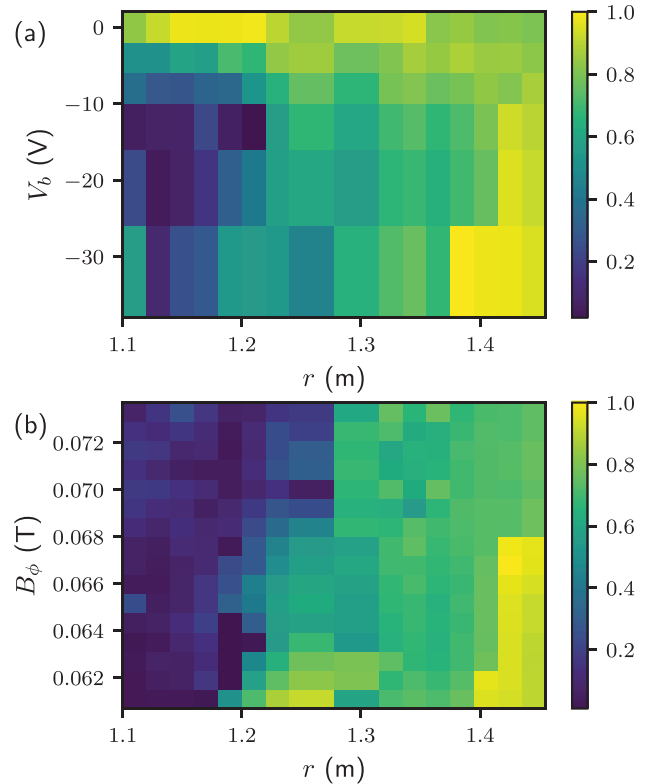


FIG. 6. The value of the parameter P_b as (a) function of the bias potential V_b and the probe radius r , and (b) of the toroidal magnetic field B_ϕ at the center of the machine ($r = 1.1$ m) and the radial position, for $V_b = -20$ V.

(bursty or burst-free) do not change, i.e., all other distribution parameters are the same as the whole time-series fitted values, and only allowed $P_b^{(w)}$ to vary freely, fitting the data by the maximum likelihood method.

In Fig. 7(a), we show the time evolution of the parameter $P_b^{(w)}$, calculated using 1.0 ms (500 points) windows, from a discharge with $V_b = -20$ V and a probe at $r = 1.25$ m. The mean value of P_b is shown in black. The $P_b^{(w)}$ values oscillate in the whole interval. Figure 7(b) shows time series used to estimate the correspondent square points from Fig. 7(a), selected as examples of bursty series ($P_b^{(w)} \approx 1$). Figure 7(c) shows series used to estimate the star points, Gaussian like series ($P_b^{(w)} \approx 0$). The signals in these two time intervals groups are remarkable different, as the one with $P_b^{(w)} \approx 1$ presents sequences of bursts with typical fast rise and decay profile and a much lower baseline density, while the burst-free (or suppressed) shows oscillation without any burst and a much higher background density.

The $P_b^{(w)}$ time series is estimated by a rather complicated procedure, thus it is necessary to develop an adequate validation procedure to take into account the experimental histogram and temporal correlations to draw conclusions on the alternation of regime behavior. A relatively simple way to create a stochastic time series that follows both the fitted distribution and the correlation times of the experimental series is by using the Metropolis–Hastings algorithm with an adequate choice of both sampling rate and candidate standard-deviation.

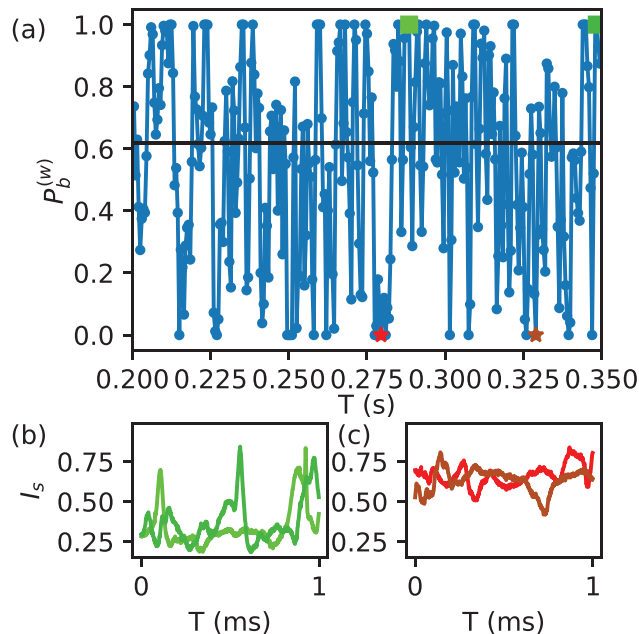


FIG. 7. (a) A time series of the estimated values of $P_b^{(w)}$, showing also the whole series value of P_b (black). (b) Examples of windows corresponding to bursty regimes in the series [square points in (a)]. (c) Windows corresponding to Gaussian regime in the series [star points in (a)].

The $P_b^{(w)}$ series calculated from experimental data has its histogram and correlation profiles compatible with both a stochastic simulation (obtained from a Metropolis–Hastings algorithm) and an intermittent switching between the two different distributions [bursty and burst-free, described by Eq. (4)]. However, the stationary stochastic model fails to reproduce many features of the experimental series. When the conditional average of large bursts is calculated, the experimental series shows short duration pulses, a feature not reproduced by the stochastic series.

Windows of $P_b^{(w)} \approx 0$ and $P_b^{(w)} \approx 1$ have different auto-correlation profiles, and they also differ from the stochastic model ones. This result is an indication that the different $P_b^{(w)}$ values are capturing different turbulent regimes, and even if they may not be an ideal estimator of these regimes, they are able to capture some difference in the temporal properties of the series, besides not directly measuring temporal correlations. However, further analyses should be done to validate our conjecture about the regime's alternation.

VI. CONCLUSION

We investigated the turbulence of the Texas Helimak plasma. In the usual conditions, the low field side of the average plasma density peak presents a turbulence that is characterized by the presence of many high-density bursts. This bursty regime generates a characteristic skewed distribution in the ion saturation signals. When we apply a negative electrostatic bias, the turbulence regime changes in the vicinity of the biasing plate, going to a burst-free turbulence with Gaussian distribution.

While the region close to where the bias is applied changes the turbulence regime, the far low field side region is almost unaffected by

the biasing, keeping a burst dominated turbulence. The presence of two regimes in different regions of the machine allowed us to study the spatial transition between them by analyzing the signals from probes at different radial positions. This transition is analogue to the one observed in fusion machines when going from inside the plasma column to the scrape-off layer.

We found that the turbulence at the regime transition region can be described as a coexistence between the two limit case regimes: a burst-free with Gaussian fluctuation, in which the bursts are suppressed and the plasma density is increased, and a bursty regime composed of a stochastic burst train, with random burst occurrence times, exponential amplitude distributions and double exponential temporal profile. The transition is compatible with a change in the amount of time that the turbulence stays in each regime, going from always in the burst-free regime, for smaller radial positions, to always in the bursty regime, for large radial positions.

The large bursts present in the bursty turbulence regime makes the density achieve higher values than in the burst-free regime for short time intervals. However, the transition between burst-free and bursty turbulence imposes a decrease in the mean plasma density. This agrees with the notion that the bursts presence is associated with an increase in the plasma transport and/or particle loss. The regime coexistence scenario identified may open interesting perspectives on the understanding of the burst formation process and its effect on the particle transport.

ACKNOWLEDGMENTS

We would like to acknowledge financial support from the Brazilian agencies: São Paulo Research Foundation (FAPESP)-Grant Nos. 2015/50122-0, 2017/23128-3, and 2018/03211-6 and CNPq-Grant Nos. 141192/2016-0, 302665/2017-0, 407299/2018-1, and 156067/2018-8.

DATA AVAILABILITY

The data that support the findings of this study are available from the corresponding author upon reasonable request.

REFERENCES

- C. W. Horton, Jr. and S. Benkadda, *ITER Physics* (World Scientific, 2015).
- C. Hidalgo, *Plasma Phys. Controlled Fusion* **37**, A53 (1995).
- W. Horton, *Turbulent Transport in Magnetized Plasmas*, 2nd ed. (World Scientific, 2018).
- G. Y. Antar, S. I. Krasheninnikov, P. Devynck, R. P. Doerner, E. M. Hollmann, J. A. Boedo, S. C. Luckhardt, and R. W. Conn, *Phys. Rev. Lett.* **87**, 065001 (2001).
- G. Y. Antar, G. Counsell, Y. Yu, B. Labombard, and P. Devynck, *Phys. Plasmas* **10**, 419 (2003).
- S. I. Krasheninnikov, D. A. D'Ippolito, and J. R. Myra, *J. Plasma Phys.* **74**, 679 (2008).
- R. Kube, A. Theodorsen, O. E. Garcia, B. LaBombard, and J. L. Terry, *Plasmas Phys. Controlled Fusion* **58**, 054001 (2016).
- T. A. Carter, *Phys. Plasmas* **13**, 010701 (2006).
- D. L. Toufen, F. A. C. Pereira, Z. O. Guimarães-Filho, I. L. Caldas, and K. W. Gentile, *Phys. Plasmas* **21**, 122302 (2014).
- F. A. C. Pereira, D. L. Toufen, Z. O. Guimarães-Filho, I. L. Caldas, and K. W. Gentile, *Plasma Phys. Controlled Fusion* **58**, 054007 (2016).
- I. Furno, B. Labit, A. Fasoli, F. M. Poli, P. Ricci, C. Theiler, S. Brunner, A. Diallo, J. P. Graves, M. Podestà, and S. H. Müller, *Phys. Plasmas* **15**, 055903 (2008).

- ¹²K. Rypdal and S. Ratynskaia, *Phys. Rev. Lett.* **94**, 225002 (2005).
- ¹³S. J. Zweben, J. A. Boedo, O. Grulke, C. Hidalgo, B. LaBombard, R. J. Maqueda, P. Scarin, and J. L. Terry, *Plasma Phys. Controlled Fusion* **49**, S1–S23 (2007).
- ¹⁴D. A. D'Ippolito, J. R. Myra, and S. J. Zweben, *Phys. Plasmas* **18**, 060501 (2011).
- ¹⁵J. E. Maggs and G. J. Morales, *Plasma Phys. Controlled Fusion* **54**, 124041 (2012).
- ¹⁶T. A. Carter and J. E. Maggs, *Phys. Plasmas* **16**, 012304 (2009).
- ¹⁷S. J. Zweben, J. R. Myra, W. M. Davis, D. A. D'Ippolito, T. K. Gray, S. M. Kaye, B. P. LeBlanc, R. J. Maqueda, D. A. Russell, D. P. Stotler, and NSTX-U Team, *Plasma Phys. Controlled Fusion* **58**, 044007 (2016).
- ¹⁸J. E. Maggs and G. J. Morales, *Phys. Rev. Lett.* **107**, 185003 (2011).
- ¹⁹O. E. Garcia, *Phys. Rev. Lett.* **108**, 265001 (2012).
- ²⁰A. Theodorsen, O. E. Garcia, R. Kube, B. LaBombard, and J. L. Terry, *Nucl. Fusion* **57**, 114004 (2017).
- ²¹J. E. Maggs and G. J. Morales, *Phys. Rev. E* **86**, 015401 © (2012).
- ²²F. A. C. Pereira, I. M. Sokolov, D. L. Toufen, Z. O. Guimarães-Filho, I. L. Caldas, and K. W. Gentle, *Phys. Plasmas* **26**, 052301 (2019).
- ²³K. W. Gentle and H. Huang, *Plasma Sci. Technol.* **10**, 284 (2008).
- ²⁴D. L. Toufen, Z. O. Guimarães-Filho, I. L. Caldas, J. D. Szezech, S. Lopes, R. L. Viana, and K. W. Gentle, *Phys. Plasmas* **20**, 022310 (2013).
- ²⁵S. Dharmadhikari and K. Joag-dev, *Unimodality, Convexity, and Applications* (Academic Press, 1988).